



VICTORIA UNIVERSITY
MELBOURNE AUSTRALIA

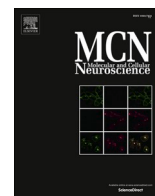
microRNA-146a modulates behavioural activity, neuroinflammation, and oxidative stress in adult mice

This is the Published version of the following publication

Zhao, Wenting, Spiers, Jereme G, Vassileff, Natasha, Khadka, Arun, Jaehne, Emily J, van den Buuse, Maarten and Hill, Andrew F (2023) microRNA-146a modulates behavioural activity, neuroinflammation, and oxidative stress in adult mice. *Molecular and Cellular Neuroscience*, 124. ISSN 1044-7431

The publisher's official version can be found at
<https://www.sciencedirect.com/science/article/pii/S1044743123000143?via%3Dihub>
Note that access to this version may require subscription.

Downloaded from VU Research Repository <https://vuir.vu.edu.au/46663/>



microRNA-146a modulates behavioural activity, neuroinflammation, and oxidative stress in adult mice

Wenting Zhao^{a,1}, Jereme G. Spiers^{a,1}, Natasha Vassileff^a, Arun Khadka^a, Emily J. Jaehne^a, Maarten van den Buuse^{b,c}, Andrew F. Hill^{a,d,*}

^a Department of Biochemistry and Genetics, La Trobe Institute for Molecular Science, La Trobe University, Bundoora, Victoria 3083, Australia

^b Department of Psychology, Counselling and Therapy, School of Psychology and Public Health, La Trobe University, Melbourne, Australia

^c Department of Pharmacology, University of Melbourne, Melbourne, Australia

^d Institute for Health and Sport, Victoria University, Footscray, Melbourne, Australia

ARTICLE INFO

Keywords:

Cytokines
Locomotor activity
miRNA
Neuroinflammation
Oxidative stress

ABSTRACT

Small non-coding miRNA act as key regulators of several physiological processes due to their ability to interact with numerous target mRNA within a network. Whilst several miRNA can act in concert to regulate target mRNA expression, miR-146a has emerged as a critical modulator of inflammation by targeting key upstream signalling proteins of the nuclear factor kappa-light-chain-enhancer of activated B cells (NF-κB) pathway and reductions in this miRNA have been observed in several neurological and neurodegenerative disorders. However, a targeted assessment of behaviour and neural tissues following the loss of miR-146a has not been documented. In this study, we examined the behavioural and neuroinflammatory phenotype of mice lacking miR-146a to determine the role of this miRNA in neurological function. Adult miR-146a^{-/-} mice displayed no overt developmental phenotype with the exception of enlarged spleens. Behavioural testing revealed a mild but significant reduction in exploratory locomotor activity and increase in anxiety-like behaviour, with no changes in short-term spatial memory, fear conditioning, or sensorimotor gating. In the brain, the lack of miR-146a resulted in a significant compensatory miR-155 expression with no significant changes in expression of the target Interleukin 1 Receptor Associated Kinase (Irak) gene family. Despite these effects on upstream NF-κB mediators, downstream expression of cytokine and chemokine messengers was significantly elevated in miR-146a^{-/-} mice compared to wild-type controls. Moreover, this increase in inflammatory cytokines was observed alongside an induction of oxidative stress, driven in part by nicotinamide adenine dinucleotide phosphate (NADPH)-oxidase, and included reduced thiol antioxidant concentrations and increased oxidised protein carbonyl concentrations. In female miR-146a mice, this increase in oxidative stress resulted in an increased expression of superoxide dismutase 1 (SOD1). Together, this suggests miR-146a plays a key role in regulating inflammation even in the absence of inflammatory stimuli and reduced levels of this miRNA have the capacity to induce limited behavioural effects whilst exacerbating both inflammation and oxidative stress in the brain.

1. Introduction

Neuroinflammation is a common feature of several neurological conditions, including neuropsychiatric and neurodegenerative disorders, often appearing very early in the pathogenesis of these diseases (Mander and Brown, 2005; Felger et al., 2016; Spiers et al., 2019; Bourgognon et al., 2021). At the cellular level, a variety of stress and inflammatory signals converge to signal via the transcription factor,

nuclear factor kappa-light-chain-enhancer of activated B cells (NF-κB) which in turn regulates inflammatory tone in part via the activation/suppression of several cytokines (Shih et al., 2015). Pro-inflammatory cytokines such as interleukin 1-beta (IL1β), interleukin 6 (IL6), and tumor necrosis factor alpha (TNF-α) subsequently exert pleiotropic effects via their cognate receptors to promote inflammation and oxidative stress (Wang et al., 2015). Due to the broad activation characteristics of NF-κB, multiple cellular processes can act as modulators of its signalling,

* Corresponding author at: Institute for Health and Sport, Victoria University, Footscray, Melbourne, Australia.

E-mail address: Andy.Hill@vu.edu.au (A.F. Hill).

¹ Contributed equally to this work.

particularly upstream of NF- κ B activation. This includes microRNA (miRNA), small non-coding 19–24 nucleotide RNAs produced by RNA polymerases II & III. Mature miRNA can bind to the 3' untranslated regions (3' UTR) of mRNA to modulate protein translational efficiency and promote transcript degradation. Conserved 3' UTR binding sites in mature mRNA allow miRNA to influence translation on a network scale, often acting on multiple targets to regulate overall activity within a pathway (Yang and Wang, 2011).

Whilst several miRNAs can modulate immune function, miR-146a has emerged as a significant regulator of inflammation, providing critical negative feedback on cytokine production by influencing targets such as Interleukin-1 receptor-associated kinase 1 (IRAK1) and TNF receptor associated factor 6 (TRAF6) upstream of NF- κ B (Walsh et al., 2015; Testa et al., 2017). Importantly, binding of the NF- κ B transcription factor to sites in the miR-146a promoter region regulates miR-146a expression, highlighting the importance of miR-146a in the homeostatic modulation of the inflammatory response (Taganov et al., 2006). Furthermore, miR-146a regulation of NF- κ B is particularly prevalent in myeloid lineage cells, including monocytes and macrophages, highlighting that expression of this miRNA is localised in key immunoregulatory cell types (Boldin et al., 2011). In the brain, this predominately includes microglia, the resident neural immune cells capable of mounting a neuroinflammatory response through a combination of cytokine and chemokine messengers. These messengers additionally mobilise a suite of oxidative stress machinery such as the cytosolic nicotinamide adenine dinucleotide phosphate (NADPH)-oxidase (NOX) that typically produces reactive superoxide radicals to protect against invading pathogens (Mander and Brown, 2005). However, unchecked superoxide production increases oxidative stress through direct interactions with protein, lipid, and nucleic acids and increases downstream reactive oxygen species (ROS) enzymatic degradation products such as hydrogen peroxide and hydroxyl radical (Spiers et al., 2015). Due to the wide-ranging targets of miRNA, very little is known about the impact of miRNA dysfunction on basal redox status in the brain. Therefore, to understand the importance of miR-146a in normal physiology, we generated a mouse model lacking this miRNA and characterised the behavioural phenotype, basal expression of inflammatory genes, and markers of general oxidative stress in the brain of middle-aged adult mice. It was hypothesised that the lack of miR-146a feedback control over upstream inflammatory NF- κ B targets would ultimately lead to a state of neuroinflammation and oxidative stress despite the absence of disease or pathogen in these mice.

2. Methods

2.1. Experimental animals

All animal procedures were in strict accordance with the Australian Code of Practice for the Care and Use of Animals for Scientific Purposes and were assessed and approved by the La Trobe University Animal Ethics Committee (AEC16-37 and AEC18-02). Mice lacking miR-146a were generated using CRISPR/Cas9 gene editing by the Australian Phenomics Network CRISPR service (Monash University, Victoria, Australia). Briefly, to deplete whole-genome miR-146a, two guide RNAs were introduced to C57BL/6 mouse zygotes. These were differentiated to blastocysts and implanted into surrogate mice. The first-generation hemizygous foundation mice (miR-146a^{+/-}) were used to further produce homozygous miR-146a^{-/-} mice. These were backcrossed with C57BL/6 mice, and heterozygotes were used to regenerate homozygous mice for use in experiments. Genotyping of offspring mice was determined using qPCR and agarose gel electrophoresis. Genomic DNA was isolated, and qPCR was performed using the GoTaq Green Master Mix (Promega, M7122) and 10 μ M of each primer (described in Table S1) through a standard Polymerase Chain Reaction (PCR). The miR-146a^{-/-} and wild-type samples were identified through agarose gel electrophoresis on a 1.5 % (w/v) agarose gel containing SYBRsafe DNA stain

(Invitrogen, S33102) and visualised using the Syngene G:Box Instrument. Experimental mice were housed in IVC cages (3–5/cage) under a 12-h light cycle (lights on at 07:00) and given ad libitum access to standard pellet food and water.

Middle-aged adult mice (aged 9–12 months) were chosen for this work based on previous studies indicating middle-aged mice are more susceptible to systemic inflammation characterised in the brain by microglial activation and because miR-146a^{-/-} mice aged >18 months develop tumours (d'Avila et al., 2018; Zhao et al., 2011). These mice underwent a battery of behavioural tests over a period of three weeks, with less stressful tests performed first and more stressful tests conducted at the end (Jaehne et al., 2017; Genders et al., 2019; Tran et al., 2021). Mice were given at least 1–2 days of rest between every behavioural test. Tests were performed in the following order: exploratory locomotor activity, elevated plus maze, Y-maze, fear conditioning, and prepulse inhibition (PPI). Twenty four hours after the last behavioural test, a subset of mice were killed via cervical dislocation, and the brain was rapidly removed, frozen on dry ice, and stored at -80 °C. Cortical and thalamic regions were dissected on dry ice for gene expression, Western blot, and oxidative stress analysis.

2.2. Open field test

Mice were placed into automated photocell arenas (Med Associates, Fairfax, VT, USA), which were 27 \times 27 cm with walls 20 cm high, with a 24 \times 24 array of photobeam sensors for detecting movement. Distance travelled was monitored for 60 min and automatically calculated in 5-min time bins.

2.3. Elevated Plus Maze

The Elevated Plus Maze (EPM) consisted of an elevated plus-shaped platform with two open and two closed arms, each with a length of 40 cm and width of 5 cm, 50 cm above the ground, with a central square section between arms. Animals were placed in the central square of the maze, facing one of the two closed arms, and allowed to explore for 5 min as previously published (Wall and Messier, 2001; Boon et al., 2010). Time spent in open and closed arms and the number of entries into arms were measured using Ethovision video tracking (Noldus, The Netherlands). Mice which spend more time in the open arms are considered to have a lesser anxiety-like phenotype.

2.4. Y-maze

The Y-maze was a Y-shaped apparatus with three arms (start arm and two test arms), each 32 cm long and 10 cm wide, with walls 15 cm high. The arms were at a 120° angle from each other. The two test arms had different black and white spatial cues on either end wall. The maze floor was covered with sawdust and cage bedding which was mixed between trials to reduce olfactory cues. Behaviour was tracked using Ethovision (Noldus, The Netherlands), which measured time spent in each arm and total distance travelled. Testing was conducted according to previously published protocols (Dellu et al., 1992; Jaehne and Baune, 2014; Notaras et al., 2016). Mice were placed in the start arm of the Y-maze for two separate sessions. During the training phase, mice were allowed to explore the maze for 10 min with one of the test arms blocked off. One hour later, they were placed back in the start arm and allowed to explore the whole Y-maze for 5 min with all three arms open. The localisation of novel and familiar arms was randomised between mice. Time spent in the novel test arm during the retention phase was used as a measure of short-term spatial recognition memory.

2.5. Fear conditioning

Fear memory was assessed using a three-day fear conditioning protocol as previously used in mice (Chen et al., 2006; Notaras et al., 2016)

using chambers equipped with shock-inducing grid floors (Med Associates, Fairfax, VT, USA). Two different conditioning contexts were used, which differed in lux, scent, bedding and structure due to a concave wall insert, and mice were pseudo-randomly assigned to one context or the other. On Day 1 mice were conditioned using three tone-shock pairings of the conditioned stimulus (CS; 30 s duration, 7500 Hz, 70 dB) with the unconditioned stimulus (US; scrambled foot-shock of 1 s duration, 0.7 mA) which co-terminated together with an inter-trial interval (ITI) of 30 s between each tone-shock pairing. 24 h later on Day 2, contextual fear memory was assessed whereby mice were returned to the same context for 5.5 min, and freezing was quantified for the final 4.5 min of the period using Video Freeze software (Med Associates). Freezing was defined as a complete lack of any movement besides breathing. 48 h following the conditioning session on Day 3, tone-elicited fear memory was assessed by placing mice in the alternate context to Day 1 and 2. Similar to Day 1, mice were presented with the CS three times (30 s duration, 30 s ITI) following a 2.5 min habituation period, however, the US was not presented. Average freezing during the three 30 s CS presentations was measured.

2.6. Prepulse Inhibition of acoustic startle

Prepulse Inhibition (PPI) was assessed as a measure of sensorimotor gating using automated SR-Lab startle chambers (San Diego Instruments, San Diego, CA, USA). Mice were placed in individual plexiglass cylinders (5 cm diameter), and the test session consisted of 104 stimulus trials as previously described (van den Buuse et al., 2011; Manning and van den Buuse, 2013; Notaras et al., 2017). Test sessions consisted of four blocks of 8115 dB startle alone pulses of 40 ms, including one block at the start and end of the session and two throughout the session. Prepulse trials consisted of a single 115 dB pulse preceded either 100 or 30 ms by a 20 ms prepulse of 2, 4, 8 or 16 dB over baseline. Throughout the session, 65 dB of background white noise was maintained. The session also included eight trials during which no sound stimulus was delivered to detect possible non-specific movements. PPI was quantified as the difference between stimulus responses during prepulse-pulse and pulse alone trials and expressed as a percentage of pulse alone responses. At the 30 ms ISI mice showed low and variable PPI and no effect of genotype; therefore results analysis will focus on the 100 ms ISI.

2.7. mRNA & miRNA expression

Tissue RNA was extracted using Qiagen miRNeasy mini kits (QIAGEN, Doncaster, Australia) according to the manufacturer's instructions. The purity of sample RNA was determined using the Agilent 2100 Bioanalyser RNA 6000 Nano kits. RNA integrity numbers (RIN) averaged 8.55 for all samples used in these experiments. A total of 1 µg of eluted RNA was reverse transcribed using a High-capacity cDNA Reverse Transcription kit (Applied Biosystems Cat#4368813) according to the manufacturer's instructions. Expression of mRNA was determined using 6-Carboxyfluorescein-labelled Taqman Assay-on-demand kits for targets outlined in Table S1 and normalised to the housekeeping genes Hprt1, Rpl13, and Actb. Relative expression was calculated using the $\Delta\Delta CT$ method using the wild-type males as controls.

Small RNA concentrations were determined using the Agilent 2100 Bioanalyser with Small RNA (5067-1548) kits (Agilent Technologies). Equal quantities of small RNA were reverse transcribed using a High-Capacity cDNA reverse transcription kit (Applied Biosystems, Foster City, CA) including pooled primers for the target miRNA of interest including miR-146a (Assay ID: 000468), miR-146b (Assay ID: 001097), and miR-155 (Assay ID: 002571). The miRNA expression was determined by Taqman gene expression 'assay on demand' assays relative to miR-26a (Assay ID: 000405), snoRNA202 (Assay ID: 001232) and U6 (Assay ID: 001973) housekeeping miRNAs and subsequently expressed as fold change compared to the wild-type male group using the $\Delta\Delta CT$

method.

2.8. Western blotting

Samples were lysed in 1× lysis buffer (1 cOmplete ULTRA protease inhibitor, 5 M NaCl, 1 % (w/v) sodium deoxycholate, 1 M Tris, and Triton X 100), incubated at 4 °C for 20 min and centrifuged at 2500 ×g, at 25 °C for 5 min. Equal amounts of protein were subsequently incubated with sodium dodecyl sulphate (SDS) loading dye containing 5 % β-mercaptoethanol and denatured at 70 °C for 10 min prior to loading on a 4–12 % Bis-Tris Plus Gel (Invitrogen) for electrophoresis. The samples were transferred to a polyvinylidene difluoride (PVDF) membrane and probed with the following primary antibodies, diluted in 2.5 % skim milk in TBS-T (0.05 % Tween): Actin (Cell Signalling, 8H10D10), IRAK1 (Cell Signalling, 4540S), SOD-1 (Enzo Life Sciences, ADI-SOD-100-D), and NOX2 (ThermoFisher, BS-3889R). The membranes were subsequently incubated with the relevant secondary antibodies: mouse IgG horseradish peroxidase (HRP) (Bio-Strategy, NA931) or rabbit IgG HRP (Bio-Strategy, NA934). Incubation of the membranes with Clarity enhanced chemiluminescence (ECL) reagent (Bio-Rad) was conducted as per the manufacturer's recommendations, followed by imaging by the ChemiDoc Touch imaging system (Bio-Rad) and analysis was performed using Image Lab 5.2.1 (Bio-Rad).

2.9. Oxidative stress analysis

Protein carbonyl modifications were determined using a commercially available 2,4-dinitrophenylhydrazine (DNPH) assay (Cat #: 10005020, Cayman Chemical). The protein carbonyl groups are covalently reacted with DNPH, and the increase in absorbance is observed at 370 nm. Protein carbonyls are then quantified using the molar absorption coefficient of 22 mM⁻¹ cm⁻¹ and corrected for sample protein concentrations incorporated into the assay. The final results were expressed as nmol per mg protein. Free thiol concentrations were determined using a commercially available Free thiol detection assay (Cat no: 700340, Cayman Chemical, Ann Arbor, MI, USA) according to the manufacturer's instructions. Free cysteine thiols were quantified using a cysteine standard curve, and results were expressed as nM/mg protein.

2.10. Protein determination

Protein levels were determined according to the manufacturer's instructions using the Pierce Bicinchoninic acid (BCA) Protein assay with bovine serum albumin (BSA) as a standard.

2.11. Statistical analysis

Statistical analysis was performed using GraphPad Prism (Version 8.2.1; GraphPad Software Inc., San Diego, CA, USA). Data were initially subjected to a ROUT test to identify significant outliers ($\alpha < 0.05$). Two-way ANOVA with Fisher's least significant difference (LSD) test was used to compare male and female wild-type and miR-146a^{-/-} mice where significant differences were observed between sexes. All normally distributed data were compared using unpaired *t*-tests whilst data with non-normal distributions were compared using Mann-Whitney tests. All data were expressed as the mean ± standard error of the mean (SEM) and $p < 0.05$ was considered statistically significant.

3. Results

3.1. Loss of miR-146a caused splenomegaly and reduced behavioural activity in middle-aged adult mice

miR-146a^{-/-} mice exhibited no overt developmental phenotype and displayed similar litter sizes and growth to wild-type animals.

Genotyping confirmed PCR products from miR-146a^{-/-} mice were approximately 380 base pairs compared to the 500 base pair products from wild-type mice (Fig. 1A). There was also no difference in body weights between genotypes for either male or female mice (Fig. 1B). Post-mortem examination of major organ weights revealed a highly significant increase of approximately 1.5-fold in spleen size relative to body weight ($p < 0.001$; Fig. 1C & D) in both sexes of the miR-146a^{-/-} mice.

To probe for differences in the overall miR-146a^{-/-} behavioural phenotype, we used a broad battery of behavioural tests capable of interrogating motor and neurological function. We observed a significant reduction in open field exploratory locomotor activity in miR-146a^{-/-} mice compared to wild type controls ($p < 0.01$; Fig. 2A). Moreover, miR146a^{-/-} mice exhibited significant reductions in the time spent in open arms ($p < 0.01$; Fig. 2B) and the number of open arm entries ($p < 0.01$; Fig. 2C) in the EPM whilst no change was observed in the total number of arm entries in the test (Fig. 2D). Subsequent assessment of short-term spatial memory using the Y-maze test also revealed no significant differences between genotypes (Fig. 2E). However, similar to the open field test, the locomotor distance travelled in the Y-maze showed a significant reduction of approximately 13 % in miR-146a^{-/-} mice compared to their wild-type controls ($p < 0.01$; Fig. 2F). Lastly, no differences were observed in either contextual or cued fear conditioning (Fig. 2G & H) or sensorimotor gating (Fig. 2I & J).

3.2. Altered expression of miR-146a primary targets and accessory modulators upregulate inflammatory mediators in the brain of miR-146a^{-/-} mice

In response to inflammatory stimuli, miR-146a, miR-146b, and miR-155 have emerged as differentially expressed key miRNA capable of transcriptionally repressing similar inflammatory targets to modulate inflammation. In addition to confirming the effectiveness of miR-146a knockout (Fig. S1A), we also examined miR-146b and miR-155 expression in the brain. Although no differences were observed in miR-146b (Fig. 3A), miR-155 expression increased in miR-146a^{-/-} mice

($p < 0.01$; Fig. 3B) compared to their wild-type controls.

Some of the key targets of miR-146a include interacting members of the Irak and Traf inflammatory signalling pathways. These proteins facilitate signal transduction from surface inflammatory receptors to mediate downstream activation of the transcription factor, NF- κ B. Although analysis of target Irak1 mRNA expression trended towards an increase, there was no statistically significant difference in either Irak1 or Irak3 expression (Fig. 3C & D). Interestingly, we observed a sex-specific divergence in the expression of IRAK1 protein levels in brain cortical tissue. Two way ANOVA showed a significant main effect of sex ($F_{(1,8)} = 132.9$, $P < 0.0001$) with a significant sex x genotype interaction ($F_{(1,8)} = 12.2$, $P = 0.0082$). Post hoc analysis showed significantly higher protein levels were found in female miR-146a^{-/-} mice ($p < 0.05$; Fig. 3E) compared to wild type controls. No significant differences were observed for either Irak2 or Traf6 mRNA expression in the brain (Fig. S1B & C). We next determined expression of copper/zinc superoxide dismutase (SOD1), the primary cytosolic enzymatic antioxidant responsible for the catalytically metabolism of superoxide radicals which is sensitive to inflammation (Fig. 3E). Western blot analysis of brain tissues showed highly sex-specific changes, with two way ANOVA revealing significant main effects of genotype ($F_{(1,8)} = 120.7$, $p < 0.0001$) and sex ($F_{(1,8)} = 279.3$, $p < 0.0001$), and a significant sex x genotype interaction ($F_{(1,8)} = 121.5$, $p < 0.0001$). Post hoc analysis showed highly significant increases in female miR-146a^{-/-} mice compared to their wild-type controls ($p < 0.001$; Fig. 3E) whilst no changes were observed in male mice.

Ultimately, any increase in signalling through inflammatory mediators via reduced inhibition from miR-146a should result in potentiated cytokine signalling as these are the endpoint effectors of inflammation. Analysis of brain inflammatory cytokines showed a significant increase in expression of Il1 β ($p < 0.001$; Fig. 4A), Il6 ($p < 0.01$; Fig. 4B), Tnf ($p < 0.01$; Fig. 4C), and Ccl2 ($p < 0.001$; Fig. 4D). Expression of Nlrp3, a critical subunit of the inflammasome responsible for activating Il1 β , also significantly increased in miR-146a^{-/-} mice ($p < 0.05$; Fig. 4E) in comparison to wild-type animals.

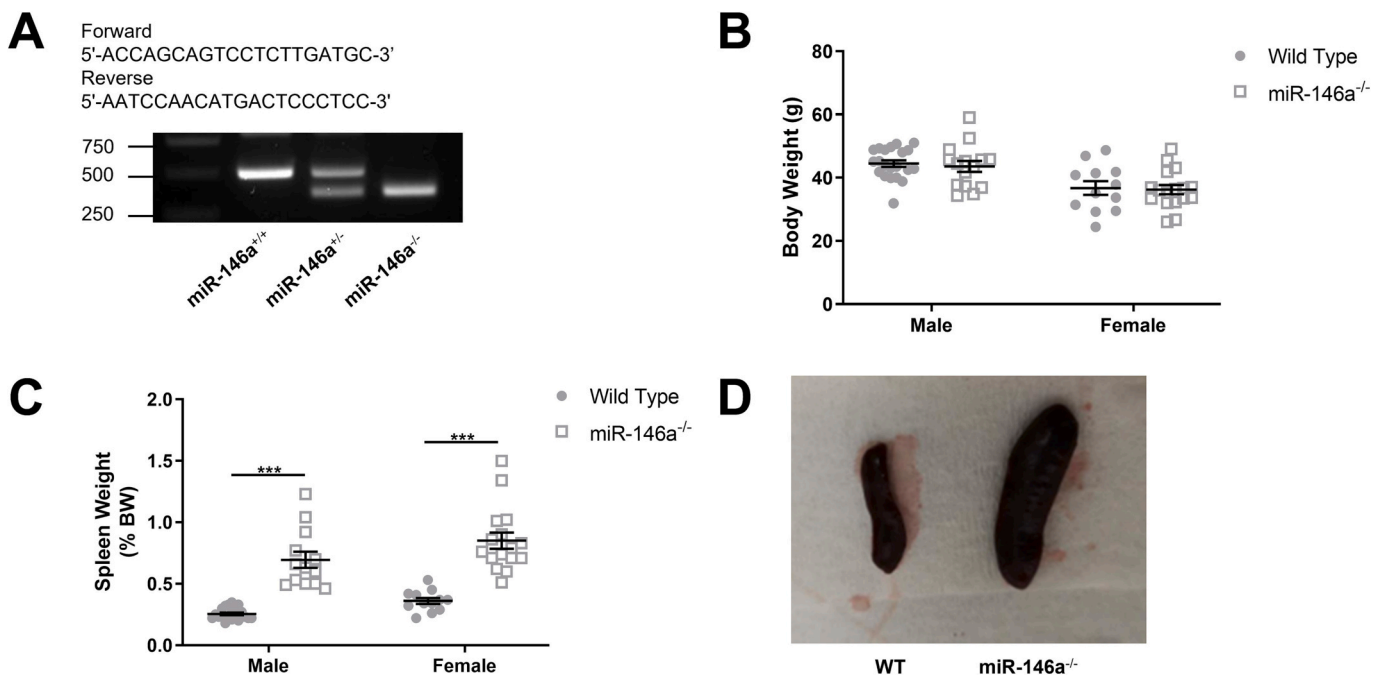


Fig. 1. Initial characterisation of miR-146a^{-/-} mice. PCR analysis of mouse genotypes shows reduced size of amplicon due to the targeted removal of miR-146a (A). No change in body weight (B) was observed in either male or female mice due to loss of miR-146a. Both male and female miR-146a^{-/-} mice displayed significant increases in relative spleen weights (C) consistent with splenomegaly (D). Body and organ weight data were compared using a two way ANOVA with Fisher's post hoc analysis and expressed as mean \pm SEM, $n = 12$ – 21 per group, *** $p < 0.001$.

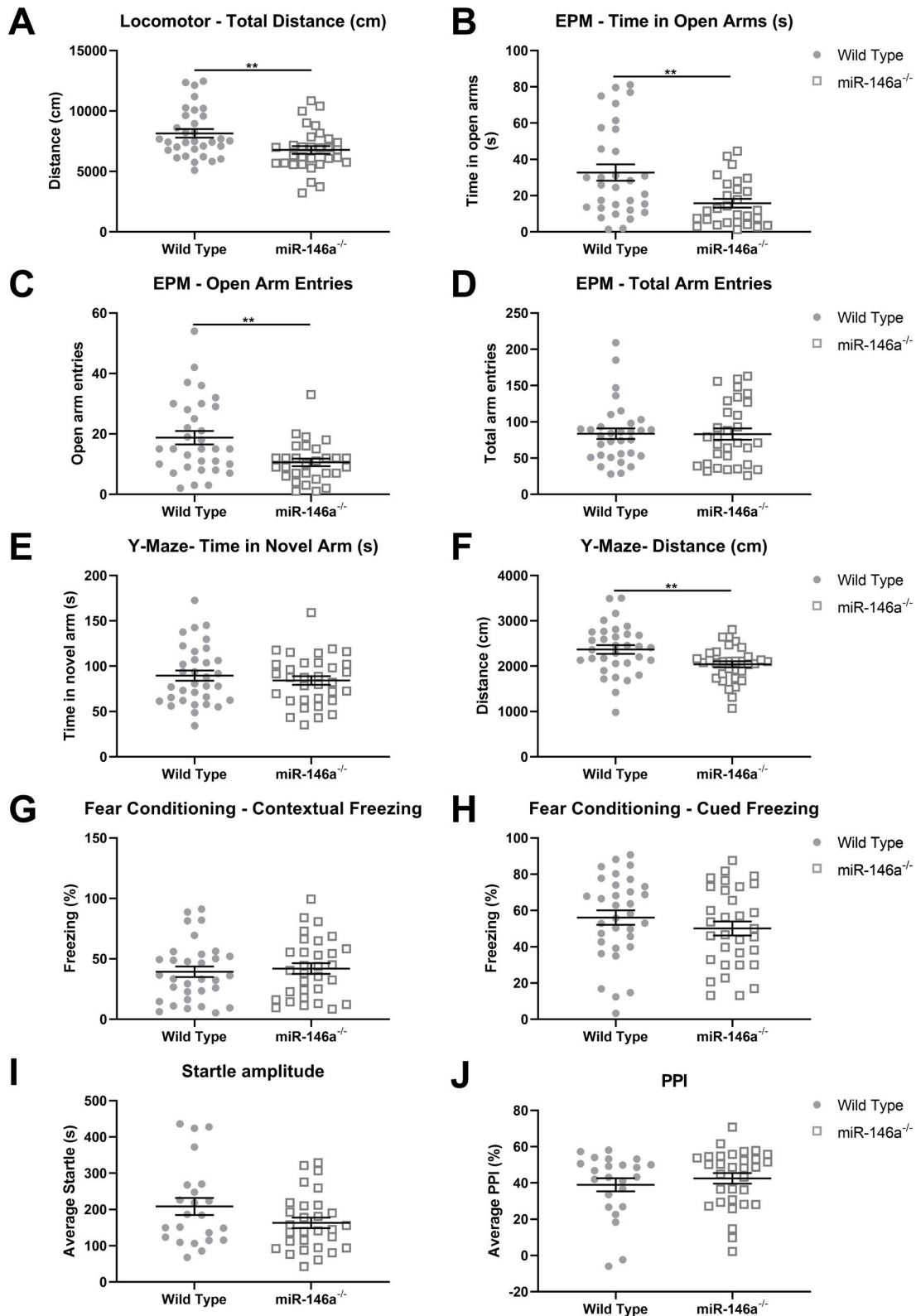


Fig. 2. Behavioural analysis of adult miR-146a^{-/-} mice. Open field activity showed reduced locomotor activity in miR-146a^{-/-} mice compared to wild type controls (A). Elevated plus maze (EPM) activity also showed reductions in time spent in the open arms (B) and the number of open arm entries (C) despite no changes being observed in the total number of arm entries (D). Analysis of Y-maze behaviour showed no change in novel arm exploration (E) whilst there was an overall reduction in Y-maze activity (F). No changes were observed in either Contextual (G) or Cued (H) freezing during fear conditioning behavioural analysis and there was no difference in sensorimotor gating in the Prepulse Inhibition (PPI) test (I & J). Behavioural data were compared using Student's *t*-tests or Mann-Whitney *U* tests and expressed as mean ± SEM, n = 28–32 per group, **p < 0.01.

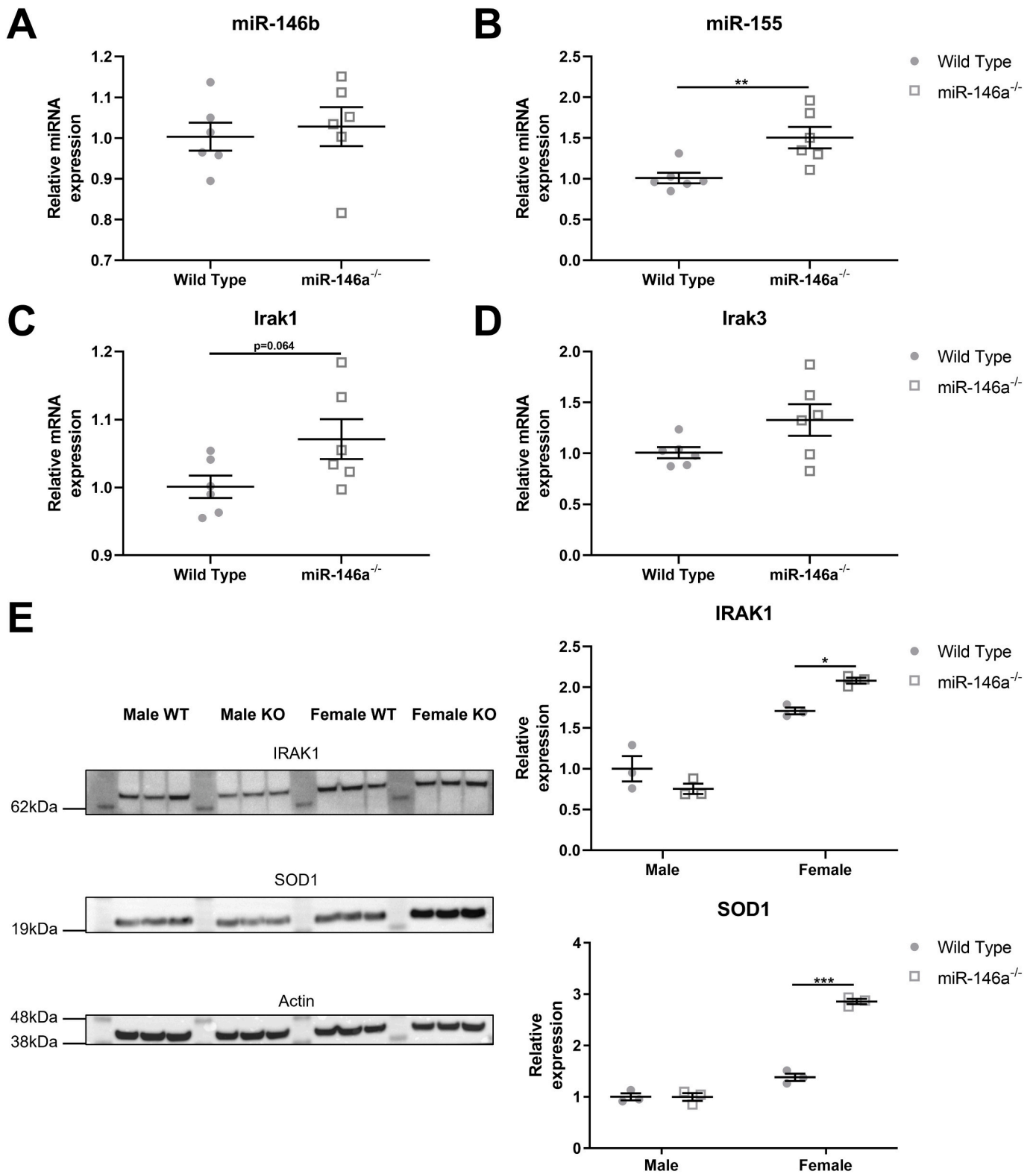


Fig. 3. Subtle changes in accessory miRNA and primary target expression in miR-146a^{-/-} mice. Loss of miR-146a had no effect on expression of miR-146b (A) and increased expression of miR-155 (B; n = 6 per group). Although there were subtle increases in target mRNA Irak1 (C) and Irak family member Irak3 (D), these did not reach statistical significance (n = 6 per group). Western blot analysis (E) showed a sex-specific divergence in expression of IRAK1 protein, with significant increases found only in female miR-146a^{-/-} mice (n = 3 per group). A sex specific increase in the antioxidant protein, SOD1, was also found in female miR-146a^{-/-} mice (n = 3 per group). MiRNA and mRNA data were compared using Student's t-tests or Mann-Whitney U tests. Protein data were compared using two way ANOVA with Fisher's post hoc analysis and expressed as mean ± SEM, *p < 0.05 and ***p < 0.01.

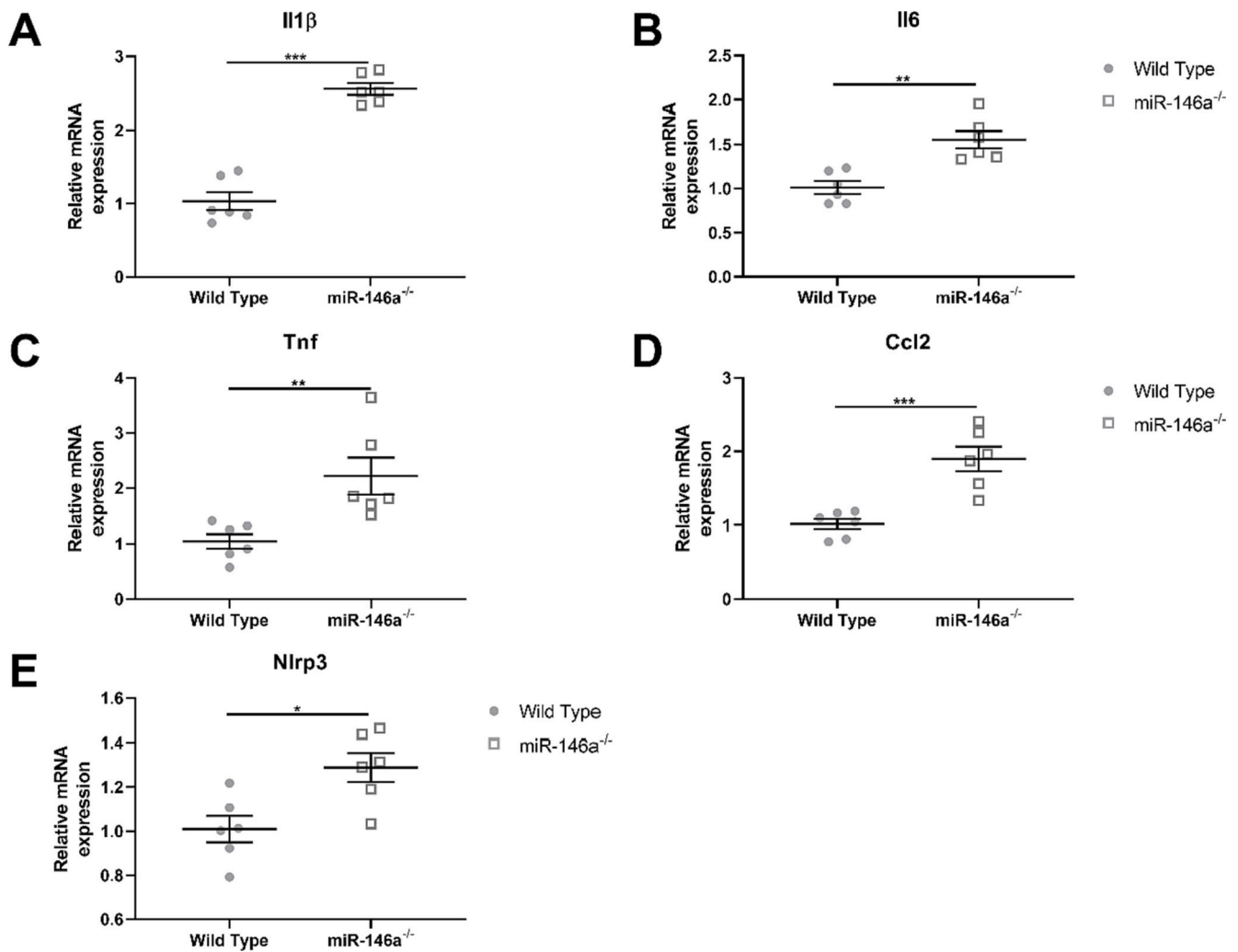


Fig. 4. Loss of miR-146a promotes proinflammatory cytokine expression. There was increased expression of Il1 β (A), Il6 (B), Tnf (C), and Ccl2 (D) mRNA in miR-146a^{-/-} mice. The inflammasome component Nlr3p mRNA was also increased in miR-146a^{-/-} mice compared to wild type controls (E). Cytokine data were compared using Student's *t*-tests and expressed as mean \pm SEM, *n* = 6 per group, **p* < 0.05, ***p* < 0.01, and ****p* < 0.001.

3.3. miR-146a^{-/-} mice displayed altered expression of superoxide radical-related enzymes and markers consistent with inflammatory oxidative stress in the brain

Inflammation is closely associated with increased oxidative stress, with both systems positively driving each other in the absence of inhibitory signalling. The increased cytokine expression in miR-146a^{-/-} mice led us to investigate oxidative stress in the brains of these mice. As a general marker of oxidative stress, we initially assayed brain tissue levels of cysteine free thiols as a proxy measure of non-enzymatic antioxidant capacity. Analysis showed significant decreases in cysteine thiol concentrations of approximately 15 % in miR-146a^{-/-} mice (*p* < 0.001; Fig. 5A). We further evaluated levels of carbonylated proteins as an indicator of direct oxidative damage to proteins, with analysis showing brain tissue protein carbonylation increased by approximately 65 % in miR-146a^{-/-} mice (*p* < 0.01; Fig. 5B). To investigate this further, we initially measured the expression of Nfe2l2 (NRF2), one of the master regulators of redox signalling. However, there was no significant difference in Nfe2l2 expression (Fig. 5C). We next measured the expression of Cybb, a critical subunit of the cytoplasmic superoxide radical generator, NADPH-oxidase, and showed increased expression in the brains of miR-146a^{-/-} mice compared to wild type controls (*p* < 0.01; Fig. 5D). Western blot for the NADPH-oxidase NOX2 subunit encoded by Cybb also showed sex-specific divergence, with two way ANOVA revealing a

significant main effect of genotype ($F_{(1,8)} = 6.342$, *P* = 0.0359) and a significant sex \times genotype interaction ($F_{(1,8)} = 5.922$, *P* = 0.041). Post hoc analysis showed significant increases in male miR-146a^{-/-} mice in comparison to their wild-type controls (*p* < 0.05; Fig. 5E). However, no difference was observed in NOX2 expression between female wild-type and miR-146a^{-/-} mice.

4. Discussion

In this study we investigated the role of miR-146a in maintaining normal brain physiology by examining the somatic and behavioural phenotype, in addition to molecular indicators of neuroinflammation and oxidative stress, in adult miR-146a^{-/-} mice. We observed distinct signs of splenomegaly, significantly reduced exploratory locomotor activity, and increased anxiety-like behaviour in the absence of other behavioural changes or any major disease-related phenotype. In the brain, the absence of miR-146a caused a generalised compensatory increase in miR-155 in addition to selectively enhancing expression of the inflammatory cytokines. This increased neuroinflammatory flux was further illustrated by an increase in mediators of oxidative stress, resulting in loss of cysteine thiols and increased protein carbonylation.

The changes in splenic growth of miR-146a^{-/-} mice are consistent with similar studies of mice lacking miR-146a/b and likely relate to the critical importance of miR-146 in regulating proliferation of myeloid

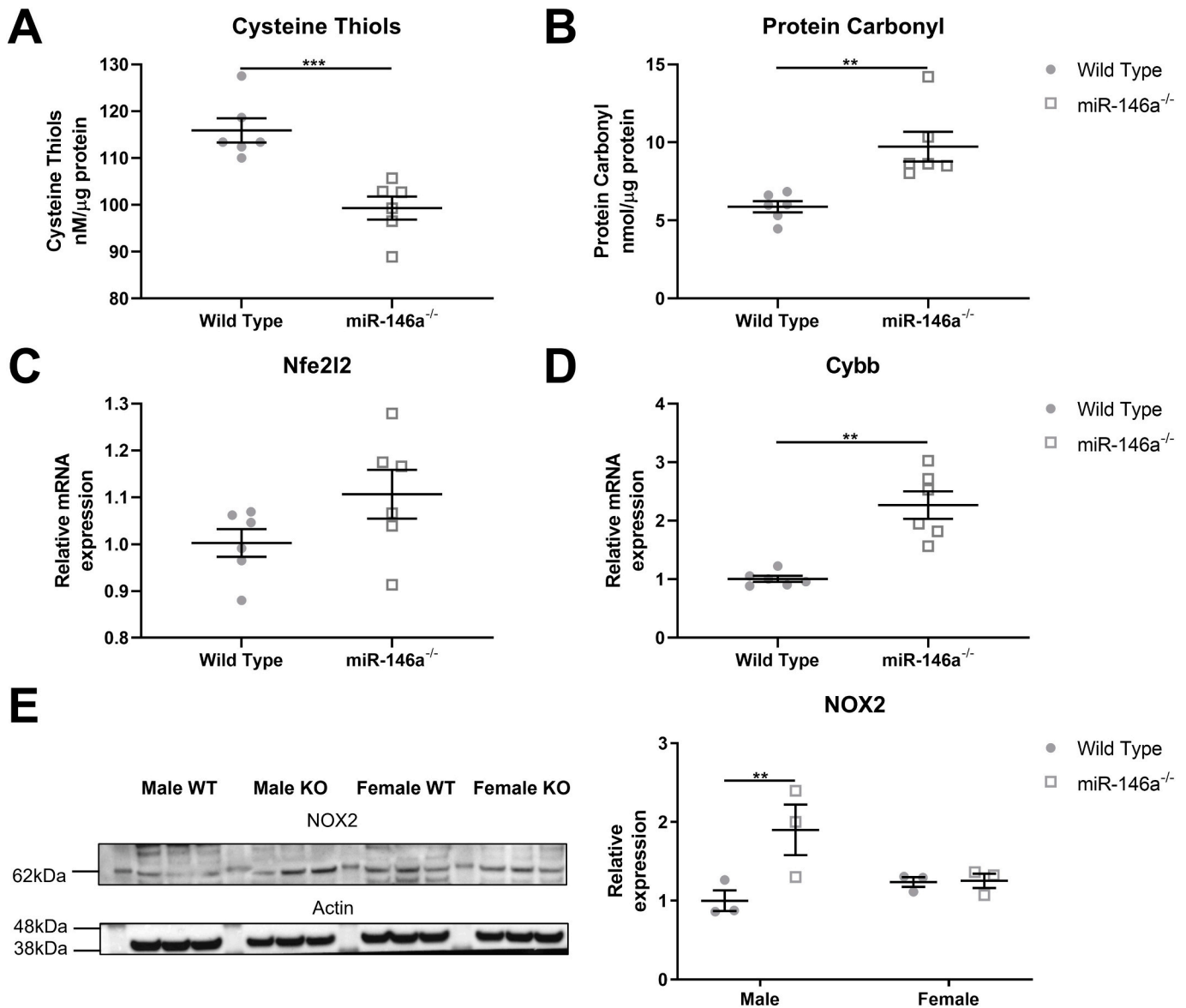


Fig. 5. miR-146a^{-/-} mice displayed increased oxidative stress. The loss of miR-146a significantly reduced the abundance of free cysteine thiols (A) and increased oxidised protein carbonyl groups (B). Although there was no change in the expression of the redox regulatory Nfe2l2 mRNA (C), there was a significant increase in subunit expression of the cytosolic superoxide radical generator, NADPH-oxidase (Cybb), in miR-146a^{-/-} mice (D; n = 6 per group). Western blot analysis showed a sex-specific increase in the catalytic NADPH-oxidase membrane bound subunit NOX2 was found in male miR-146a^{-/-} mice (E). Oxidative stress and mRNA data were compared using Student's t-tests or Mann-Whitney *U* tests. Protein data were compared using two way ANOVA with Fisher's post hoc analysis and expressed as mean \pm SEM, ***p* < 0.01 and ****p* < 0.001.

lineage cell types found in spleen tissues (Boldin et al., 2011; Zhao et al., 2011; Peng et al., 2016). Using a similar miR-146a^{-/-} mouse, Zhao and colleagues (Zhao et al., 2011) demonstrated excessive myeloproliferation, particularly of splenic and bone marrow tissues, progressed to myeloid malignancy in mice aged 18–22 months. Moreover, they subsequently showed genetic ablation of the NF- κ B p50 subunit abrogated myeloproliferation in miR-146a^{-/-} mice, suggesting overactivation of the NF- κ B inflammatory pathway is likely driving myeloid malignancy. In our middle-aged adult mice (aged 9–12 months), we only observed major changes in the spleen which houses reservoirs of myeloid cells for deployment during inflammation. In the absence of disease, it is likely that these changes arise from tissue resident macrophages found in all major organs (Nahrendorf, 2019). In addition to myeloproliferation, resident tissue macrophages in mice lacking miR-146a likely exhibit enhanced susceptibility to M1-polarisation, characterised by increased local inflammatory cytokine and ROS production via reduced repression

of the NF- κ B signalling pathway (Boldin et al., 2011; Zhao et al., 2011).

The observation of reduced open field locomotor activity and distance travelled in the Y-maze suggests an overall reduction in exploratory activity in mice lacking miR-146a. Notably, the reduced time spent in the open arms and reduced number of open arm entries by miR-146a^{-/-} mice were observed in conjunction with unchanged total number of arm entries in the EPM, suggesting the observed reductions were not confounded by reduced exploratory activity in this test. The ability of miRNA to target broad networks of mRNA makes isolating specific molecular targets responsible for behavioural modifications difficult. However, increased inflammation has also been strongly correlated with reduced motivation and motor activity (Biesmans et al., 2013; Bonsall et al., 2015; Felger and Treadway, 2017). Administration of pro-inflammatory mediators such as lipopolysaccharide or I κ B β reduces locomotor activity in mice, an effect broadly suggested to arise from reduced dopamine availability in the corticostriatal neurocircuitry

(Engeland et al., 2001; Bonsall et al., 2015). The significant inflammatory changes observed in neural tissue of naive adult miR-146a^{-/-} mice indicate these animals exhibit sustained neuroinflammation in the absence of exogenous inflammatory stimuli. This type of chronic neuroinflammation is similar to neuropsychiatric disorders such as Major Depressive Disorder where dysfunctional corticostriatal activity has been observed concurrently with inflammation and reduced motivation and motor activity (Felger et al., 2016). This may also begin to explain the observation of anxiety-like behaviour in mice lacking miR-146a as neuroinflammatory conditions, particularly those utilising Il1 β signalling, have been associated with anxiogenic behaviours (Koo and Duman, 2009). Although we did not find any differences in short-term spatial memory, fear conditioning or sensorimotor gating, it is likely that these mice are highly susceptible to experimentally induced inflammatory-related conditions which may subsequently alter these downstream behaviours. For example, exposure to chronic stress, frequently associated with the development of anxiety and depression, results in dysfunctional glucocorticoid signalling leading to the development of neuroinflammation (Chen et al., 2015; Song et al., 2020). Taken together, the reduction in locomotor activity and increased anxiety-like behaviour in miR-146a^{-/-} mice is in agreement with both experimental and clinical models of inflammation and likely stems from the broader inflammatory phenotype displayed by these mice. Further experimental models/treatments in these mice may be used to uncover the specific circuitry susceptible to the neuroinflammatory reductions in activity observed in the absence of miR-146a.

It has been well documented that miR-146a targets members of the Irak/Traf signalling pathway, with genetic ablation of miR-146a therefore predicted to increase inflammatory flux through these pathways (Taganov et al., 2006; Hou et al., 2009; Boldin et al., 2011). However, fine tuning the inflammatory response is achieved through multiple miRNA including miR-146b and miR-155. Although miR-146a, miR-146b, and miR-155 are derived from separate genetic loci, their expression is driven by a number of common inflammatory stimuli (Testa et al., 2017). Whilst miR-146a and miR-146b share a seed sequence and therefore repress overlapping inflammatory targets, miR-155 generally targets effectors to promote inflammation by increasing cytokine production pathways (Testa et al., 2017). In the present study, knockout of miR-146a did not alter expression of miR-146b in cortical tissues. However, miR-155 showed a significant increase in miR-146a^{-/-} mice. Upregulation of miR-155 generally drives inflammation via various cell types and pathways including but not limited to promoting macrophage M1 polarisation and neutrophil activation with subsequent extracellular trap formation (Cai et al., 2012; Hawez et al., 2019). In addition to promoting NF- κ B signalling, the splenic myeloproliferation contributing to splenomegaly may be facilitated by a compensatory increase in miR-155 which becomes activated in the development of several malignancies and is abundantly expressed in the spleen (Testa et al., 2017). Given the loss of inflammatory repression exerted by miR-146a, we expected to see increased inflammatory drive in brain cortical tissues due to reduced repression of Irak/Traf mediators. However, in our unchallenged mice, we did not observe changes in Traf6, the expected target of miR-146a. Moreover, increases in Irak1 expression in miR-146a^{-/-} mice did not reach statistical significance and no changes were observed in Irak2 or Irak3. Despite displaying limited modulation on members of the Irak family, mice lacking miR-146a displayed robust increases in downstream cytokine and chemokine expression. This latter change is in agreement with the findings of Zhao and colleagues (Zhao et al., 2011) and Boldin and colleagues (Boldin et al., 2011) who demonstrated similar increases in Tnf and Il6 in splenic tissue of mice following knockout of miR-146a. Taken together, whilst compensatory mechanisms may ameliorate some changes due to the loss of miR-146a, reduced expression of this miRNA promotes an inflammatory phenotype, most notably by increasing expression of the terminal cytokine and chemokine messengers.

Lastly, the strong increase in expression of pro-inflammatory

cytokines was also accompanied by induction of oxidative stress in brain cortical tissues. Reduced glutathione, the major non-enzymatic antioxidant, is the largest contributor to the cellular free cysteine thiol pool, with decreases in miR-146a^{-/-} mice indicating oxidation and an overall impaired ability to neutralise ROS. Moreover, we also observed increased protein carbonylation, a direct indicator of oxidative protein damage in these mice. Despite displaying clear markers of oxidative stress, miR-146a^{-/-} mice did not show any pronounced induction of NRF2 (Nfe2l2), the master regulator of redox homeostasis and antioxidant defence. This may be in part due to the increase in miR-155 which can directly target Nfe2l2 (Onodera et al., 2017). Cellular sources of excessive ROS such as NADPH-oxidase, of which Nox2 (Cybb) forms the catalytic subunit, become activated under inflammatory conditions to produce superoxide radical as part of the respiratory burst (Spiers et al., 2015). The increased expression of Nox2 observed in miR-146a^{-/-} mice is likely a direct result of the increased pro-inflammatory cytokine expression. This activation of Nox2 by inflammatory cytokines has been well documented and is one of the key mechanisms linking inflammation to oxidative stress (Mander and Brown, 2005; Hernández-Espinosa et al., 2019). Moreover, NADPH oxidase-induced oxidative stress in the brain is exacerbated by the membrane associated androgen receptor activation which may explain the higher NOX2 induction observed in male mice lacking miR-146a (Tenkorang et al., 2019). This excessive oxidative stress induced by NADPH-oxidase activity likely contributes to a feedforward inflammatory loop that further exacerbates cytokine expression (Hernández-Espinosa et al., 2019). Under normal conditions, excessive cytosolic superoxide radical is catalytically dismutated by SOD1 to form less toxic hydrogen peroxide which is further metabolised to water by peroxidase enzymes such as catalase (Spiers et al., 2015). However, inflammatory-driven increases in superoxide radical production via NADPH-oxidase overwhelm SOD1 antioxidant capacity, resulting in reductions of non-enzymatic thiol antioxidants and increased oxidation of cellular proteins such as those observed in miR-146a^{-/-} mice. SOD1 expression can be stimulated via NRF2 and NF- κ B by interacting directly with antioxidant response elements and p65- NF- κ B binding sites in the promoter region of the SOD1 gene (Rao et al., 2011). Interestingly, increased SOD1 was only observed in female miR-146a^{-/-} mice, likely due to the increased sensitivity of SOD1 expression conferred by 17 β -estradiol in the brain. Both inflammation and oxidative stress promote acute activation of neuroprotective gene networks that promote neuronal survival through antioxidant protection and sirtuin-mediated DNA repair (Calabrese et al., 2007; Calabrese et al., 2010). However, during aging, reductions in both NRF2 and sirtuin expression promote microglial activation, resulting in a neuro-inflammatory phenotype that potentiates oxidative stress. Critically, miR-146 sits central to a number of key target proteins in this network (Satoh et al., 2017; Schmidlin et al., 2019). Taken together, despite the absence of an inflammatory challenge, mice lacking miR-146a exhibited strong changes in oxidative stress that induced an increase in SOD1 antioxidant protection in female miR-146a^{-/-} mice. The high association of inflammation with oxidative stress further highlights the pro-inflammatory phenotype in the brain of mice lacking miR-146a.

In conclusion, miR-146a is a critical regulator of inflammation in the brain, acting to repress the expression of inflammatory mediators within the NF- κ B signalling pathway that ultimately regulate expression of terminal proinflammatory cytokines and chemokines. In the absence of miR-146a, mice display subtle behavioural adaptations in activity that are consistent with an inflammatory phenotype and cortical expression of pro-inflammatory cytokines induces significant oxidative stress that includes both loss of antioxidant protection and direct protein oxidation. The key role of miR-146a in regulating these neuroinflammatory processes makes this an attractive target for further exploration in neurological conditions where inflammation contributes to disease pathogenesis.

Funding details

This work was supported by the National Health and Medical Research Council Australia under Grant [GNT1132604]. This funding body had no further role in the study design; in the collection, analysis and interpretation of data; in the writing of the report; and in the decision to submit the paper for publication.

CRedit authorship contribution statement

W.Z., J.G.S., N.V., and A.K. performed experiments. E.J., M.V.B., and A.F.H. provided technical expertise and data interpretation. W.Z. and J.G.S. wrote the first draft of the manuscript.

Declaration of competing interest

The authors report there are no competing interests to declare.

Data availability

Data will be made available on request.

Acknowledgements

The authors would like to thank the staff and technicians at the La Trobe Animal Research and Teaching Facility for their assistance with animal husbandry. The mutant mice were produced via CRISPR/Cas9 oocyte injection by Monash University as a node of the Australian Phenomics Network (APN). The APN is supported by the Australian Government Department of Education through the National Collaborative Research Infrastructure Strategy, the Super Science Initiative and the Collaborative Research Infrastructure Scheme.

Appendix A. Supplementary data

Supplementary data to this article can be found online at <https://doi.org/10.1016/j.mcn.2023.103820>.

References

- d'Avila, J.C., Siqueira, L.D., Mazerand, A., Azevedo, E.P., Foguel, D., Castro-Faria-Neto, H.C., Sharshar, T., Chretien, F., Bozza, F.A., 2018. Age-related cognitive impairment is associated with long-term neuroinflammation and oxidative stress in a mouse model of episodic systemic inflammation. *J. Neuroinflamm.* 15 (1), 28.
- Biesmans, S., Meert, T.F., Bouwknecht, J.A., Acton, P.D., Davoodi, N., De Haes, P., Kuijlaars, J., Langlois, X., Matthews, L.J., Ver Donck, L., Hellings, N., Nuydens, R., 2013. Systemic immune activation leads to neuroinflammation and sickness behavior in mice. *Mediat. Inflamm.* 2013, 271359.
- Boldin, M.P., Taganov, K.D., Rao, D.S., Yang, L., Zhao, J.L., Kalwani, M., Garcia-Flores, Y., Luong, M., Devrekanli, A., Xu, J., Sun, G., Tay, J., Linsley, P.S., Baltimore, D., 2011. miR-146a is a significant brake on autoimmunity, myeloproliferation, and cancer in mice. *J. Exp. Med.* 208, 1189–1201.
- Bonsall, D.R., Kim, H., Tocci, C., Ndiaye, A., Petronzio, A., McKay-Corkum, G., Molyneux, P.C., Scammell, T.E., Harrington, M.E., 2015. Suppression of locomotor activity in female C57Bl/6J mice treated with interleukin-1 β : investigating a method for the study of fatigue in laboratory animals. *PLoS one* 10, e0140678.
- Boon, W.C., van den Buuse, M., Wegener, N., Martin, S., Chua, H.K., Bush, A.L., Masters, C.L., Adlard, P.A., Li, Q.X., 2010. Behavioural phenotype of APPC100. V717F transgenic mice over-expressing a mutant abeta-bearing fragment is associated with reduced NMDA receptor density. *Behav. Brain Res.* 209, 27–35.
- Bourgognon, J.M., Spiers, J.G., Robinson, S.W., Scheiblich, H., Glynn, P., Ortori, C., Bradley, S.J., Tobin, A.B., Steinert, J.R., 2021. Inhibition of neuroinflammatory nitric oxide signaling suppresses glycation and prevents neuronal dysfunction in mouse prion disease. *Proc. Natl. Acad. Sci. U. S. A.* 118.
- Cai, X., Yin, Y., Li, N., Zhu, D., Zhang, J., Zhang, C.Y., Zen, K., 2012. Re-polarization of tumor-associated macrophages to pro-inflammatory M1 macrophages by microRNA-155. *J. Mol. Cell Biol.* 4, 341–343.
- Calabrese, V., Guagliano, E., Sapienza, M., Panebianco, M., Calafato, S., Puleo, E., Pennisi, G., Mancuso, C., Butterfield, D.A., Stella, A.G., 2007. Redox regulation of cellular stress response in aging and neurodegenerative disorders: role of vitagenes. *Neurochem. Res.* 32, 757–773.
- Calabrese, V., Cornelius, C., Dinkova-Kostova, A.T., Calabrese, E.J., Mattson, M.P., 2010. Cellular stress responses, the hormesis paradigm, and vitagenes: novel targets for therapeutic intervention in neurodegenerative disorders. *Antioxid. Redox Signal.* 13, 1763–1811.
- Chen, Z.Y., Jing, D., Bath, K.G., Ieraci, A., Khan, T., Siao, C.J., Herrera, D.G., Toth, M., Yang, C., McEwen, B.S., Hempstead, B.L., Lee, F.S., 2006. Genetic variant BDNF (Val66Met) polymorphism alters anxiety-related behavior. *Science* 314, 140–143.
- Chen, H.-J.C., Spiers, J.G., Sernia, C., Lavidis, N.A., 2015. Response of the nitrenergic system to activation of the neuroendocrine stress axis. *Front. Neurosci.* 9.
- Dellu, F., Mayo, W., Cherkaoui, J., Le Moal, M., Simon, H., 1992. A two-trial memory task with automated recording: study in young and aged rats. *Brain Res.* 588, 132–139.
- Engeland, C.G., Nielsen, D.V., Kavaliers, M., Ossenkopp, K.P., 2001. Locomotor activity changes following lipopolysaccharide treatment in mice: a multivariate assessment of behavioral tolerance. *Physiol. Behav.* 72, 481–491.
- Felger, J.C., Treadway, M.T., 2017. Inflammation effects on motivation and motor activity: role of dopamine. *Neuropsychopharmacology* 42, 216–241.
- Felger, J.C., Li, Z., Haroon, E., Woolwine, B.J., Jung, M.Y., Hu, X., Miller, A.H., 2016. Inflammation is associated with decreased functional connectivity within corticostriatal reward circuitry in depression. *Mol. Psychiatry* 21, 1358–1365.
- Genders, S.G., Scheller, K.J., Jaehne, E.J., Turner, B.J., Lawrence, A.J., Brunner, S.M., Kofler, B., van den Buuse, M., Djouma, E., 2019. GAL(3) receptor knockout mice exhibit an alcohol-preferring phenotype. *Addict. Biol.* 24, 886–897.
- Hawez, A., Al-Haidari, A., Madhi, R., Rahman, M., Thorlacius, H., 2019. MiR-155 regulates PAD4-dependent formation of neutrophil extracellular traps. *Front. Immunol.* 10, 2462.
- Hernández-Espinosa, D.R., Massieu, L., Montiel, T., Morán, J., 2019. Role of NADPH oxidase-2 in the progression of the inflammatory response secondary to striatum excitotoxic damage. *J. Neuroinflammation* 16, 91.
- Hou, J., Wang, P., Lin, L., Liu, X., Ma, F., An, H., Wang, Z., Cao, X., 2009. MicroRNA-146a feedback inhibits RIG-I-dependent type I IFN production in macrophages by targeting TRAF6, IRAK1, and IRAK2. *J. Immunol.* 183, 2150–2158.
- Jaehne, E.J., Baune, B.T., 2014. Effects of chemokine receptor signalling on cognition-like, emotion-like and sociability behaviours of CCR6 and CCR7 knockout mice. *Behav. Brain Res.* 261, 31–39.
- Jaehne, E.J., Ameti, D., Paiva, T., van den Buuse, M., 2017. Investigating the role of serotonin in methamphetamine psychosis: unaltered behavioral effects of chronic methamphetamine in 5-HT(1A) knockout mice. *Front. Psychiatry* 8, 61.
- Koo, J.W., Duman, R.S., 2009. Interleukin-1 receptor null mutant mice show decreased anxiety-like behavior and enhanced fear memory. *Neurosci. Lett.* 456, 39–43.
- Mander, P., Brown, G.C., 2005. Activation of microglial NADPH oxidase is synergistic with glial iNOS expression in inducing neuronal death: a dual-key mechanism of inflammatory neurodegeneration. *J. Neuroinflammation* 2, 20.
- Manning, E.E., van den Buuse, M., 2013. BDNF deficiency and young-adult methamphetamine induce sex-specific effects on prepulse inhibition regulation. *Front. Cell. Neurosci.* 7, 92.
- Nahrendorf, M., 2019. Myeloid cells in cardiovascular organs. *J. Intern. Med.* 285, 491–502.
- Notaras, M., Hill, R., Gogos, J.A., van den Buuse, M., 2016. BDNF Val66Met genotype determines hippocampus-dependent behavior via sensitivity to glucocorticoid signaling. *Mol. Psychiatry* 21, 730–732.
- Notaras, M.J., Hill, R.A., Gogos, J.A., van den Buuse, M., 2017. BDNF Val66Met genotype interacts with a history of simulated stress exposure to regulate sensorimotor gating and startle reactivity. *Schizophr. Bull.* 43, 665–672.
- Onodera, Y., Teramura, T., Takehara, T., Obora, K., Mori, T., Fukuda, K., 2017. miR-155 induces ROS generation through downregulation of antioxidant-related genes in mesenchymal stem cells. *Aging Cell* 16, 1369–1380.
- Peng, L., Zhang, H., Hao, Y., Xu, F., Yang, J., Zhang, R., Lu, G., Zheng, Z., Cui, M., Qi, C. F., Chen, C., Wang, J., Hu, Y., Wang, D., Pierce, S., Li, L., Xiong, H., 2016. Reprogramming macrophage orientation by microRNA 146b targeting transcription factor IRF5. *EBioMedicine* 14, 83–96.
- Rao, A.K., Dietrich, A.K., Ziegler, Y.S., Nardulli, A.M., 2011. 17 β -estradiol-mediated increase in Cu/Zn superoxide dismutase expression in the brain: a mechanism to protect neurons from ischemia. *J. Steroid Biochem. Mol. Biol.* 127, 382–389.
- Satoh, A., Imai, S.-i., Guarente, L., 2017. The brain, sirtuins, and ageing. *Nat. Rev. Neurosci.* 18, 362–374.
- Schmidlin, C.J., Dodson, M.B., Madhavan, L., Zhang, D.D., 2019. Redox regulation by NRF2 in aging and disease. *Free Radic. Biol. Med.* 134, 702–707.
- Shih, R.H., Wang, C.Y., Yang, C.M., 2015. NF-kappaB signaling pathways in neurological inflammation: a mini review. *Front. Mol. Neurosci.* 8, 77.
- Song, A.Q., Gao, B., Fan, J.J., Zhu, Y.J., Zhou, J., Wang, Y.L., Xu, L.Z., Wu, W.N., 2020. NLRP1 inflammasome contributes to chronic stress-induced depressive-like behaviors in mice. *J. Neuroinflammation* 17, 178.
- Spiers, J.G., Chen, H.-J.C., Sernia, C., Lavidis, N.A., 2015. Activation of the hypothalamic-pituitary-adrenal stress axis induces cellular oxidative stress. *Front. Neurosci.* 8.
- Spiers, J.G., Chen, H.-J.C., Bourgognon, J.-M., Steinert, J.R., 2019. Dysregulation of stress systems and nitric oxide signaling underlies neuronal dysfunction in Alzheimer's disease. *Free Radic. Biol. Med.* 134, 468–483.
- Taganov, K.D., Boldin, M.P., Chang, K.J., Baltimore, D., 2006. NF-kappaB-dependent induction of microRNA miR-146, an inhibitor targeted to signaling proteins of innate immune responses. *Proc. Natl. Acad. Sci. U. S. A.* 103, 12481–12486.
- Tenkorang, M.A.A., Duong, P., Cunningham, R.L., 2019. NADPH oxidase mediates membrane androgen receptor-induced neurodegeneration. *Endocrinology* 160, 947–963.
- Testa, U., Pelosi, E., Castelli, G., Labbaye, C., 2017. miR-146 and miR-155: two key modulators of immune response and tumor development. *Noncoding RNA* 3.

- Tran, S.C., Jaehne, E.J., Dye, L.E., Wong, J., Bakas, J.S., Gasperoni, J.G., Hale, M.W., van den Buuse, M., Dworkin, S., Grommen, S.V.H., De Groef, B., 2021. Effect of pleomorphic adenoma gene 1 deficiency on selected behaviours in adult mice. *Neuroscience* 455, 30–38.
- van den Buuse, M., Ruimschotel, E., Martin, S., Risbrough, V.B., Halberstadt, A.L., 2011. Enhanced effects of amphetamine but reduced effects of the hallucinogen, 5-MeO-DMT, on locomotor activity in 5-HT(1A) receptor knockout mice: implications for schizophrenia. *Neuropharmacology* 61, 209–216.
- Wall, P.M., Messier, C., 2001. Methodological and conceptual issues in the use of the elevated plus-maze as a psychological measurement instrument of animal anxiety-like behavior. *Neurosci. Biobehav. Rev.* 25, 275–286.
- Walsh, M.C., Lee, J., Choi, Y., 2015. Tumor necrosis factor receptor- associated factor 6 (TRAF6) regulation of development, function, and homeostasis of the immune system. *Immunol. Rev.* 266, 72–92.
- Wang, W.Y., Tan, M.S., Yu, J.T., Tan, L., 2015. Role of pro-inflammatory cytokines released from microglia in Alzheimer's disease. *Ann. Transl. Med.* 3, 136.
- Yang, Z., Wang, L., 2011. Regulation of microRNA expression and function by nuclear receptor signaling. *Cell Biosci* 1, 31.
- Zhao, J.L., Rao, D.S., Boldin, M.P., Taganov, K.D., O'Connell, R.M., Baltimore, D., 2011. NF-kappaB dysregulation in microRNA-146a-deficient mice drives the development of myeloid malignancies. *Proc. Natl. Acad. Sci. U. S. A.* 108, 9184–9189.